

## X-ray photoemission spectra of core levels in Ni metal

L. A. Feldkamp and L. C. Davis

*Research Staff, Ford Motor Company, Dearborn, Michigan 48121*

(Received 26 February 1980)

The x-ray photoemission spectrum of a core level in Ni metal is calculated and compared to experimental results. The model is based upon a local interaction of the  $3d$  bands with the core hole. The strength of the interaction  $U$  is taken to be 4 eV, which gives a satellite binding energy approximately 6 eV greater than that of the main line. The Ni band structure is described by a linear combination of atomic orbitals method, and hybridization of the  $3d$  bands with the  $4s$ - $4p$  bands is included. The resulting spectrum is a convolution of single-band spectra (one for each  $3d$  orbital:  $xy$ ,  $yz$ , etc.). Comparison of our essentially exact numerical results to asymptotic theory is made.

### I. INTRODUCTION

The core x-ray photoemission (XPS) spectrum of a narrow-band metal consists of two parts: a main line and a satellite at higher binding energy. Hüfner and Wertheim<sup>1</sup> have measured the  $2p_{1/2}$ ,  $2p_{3/2}$ ,  $3s$ , and  $3p$  core spectra in Ni and in each case found satellite structure at  $\sim 6$  eV from the main line. Kowalczyk<sup>2</sup> found similar, but generally weaker, satellite features in other  $3d$  transition metals. The asymmetry of the main line in Ni is large, indicating that final-state interactions are important.<sup>3</sup> Hüfner and Wertheim have interpreted the satellite structure as being due to the creation of a localized  $3d$  hole on the site of the core hole. In Cu, on the other hand, the main-line asymmetry is small<sup>4</sup> and the satellite structure is negligible.<sup>2</sup> The important difference between Cu and Ni in this regard is the filling of the  $3d$  bands: In Cu, there are essentially no  $3d$  holes to interact with the core hole.

Kotani and Toyozawa<sup>5</sup> have reproduced these features qualitatively with a model in which a localized  $d$  level, close to the Fermi energy, is pulled down by the core hole. This level interacts via the  $s$ - $d$  interaction with the  $s$  electrons, giving rise to a main-line asymmetry of the type described by Doniach and Sunjic.<sup>6</sup> The  $d$  level is occupied in the final states which make up the main line but is unoccupied in the satellite.

It is our view that this model is only partially correct. Pulling down a  $d$  level (by the core hole) which is occupied in the main line, but unoccupied in the satellite, is reasonable. However, we believe the  $s$ - $d$  interaction does not play such a direct role. In this paper, we analyze a model based upon the interaction of partially filled, narrow bands interacting with the core hole. The  $s$ - $d$  interaction plays only a minor role in this model: hybridization of the bands and the resultant modification of the  $d$  density of states. A

more crucial factor is treatment of the occupancy of the  $d$  bands in the ground state, which is omitted from the Kotani-Toyozawa model.

Recently, Tersoff, Falicov, and Penn<sup>7,8</sup> have proposed a model which is similar to that discussed here. The physical mechanism is, in fact, the same but the analysis differs in some important aspects. Their work is based upon a  $t$ -matrix approximation, whereas ours is based upon exact numerical calculations. Owing to an error in their calculation, the binding energy of the satellite relative to the main line is roughly twice as large (for the same strength of interaction) as we find. In addition, we discuss the asymmetry of the main line and the applicability of asymptotic theory (Doniach-Sunjic form).

The approach we take (as opposed to the model) is based upon numerical evaluation of finite systems and is similar to that first used by Kotani and Toyozawa.<sup>5</sup> Dow and collaborators<sup>9</sup> have applied these methods to the x-ray edge singularity (absorption and emission) as well as photoemission. In that work, the emphasis was primarily on free-electron metals and the validity of the asymptotic theory of Nozières and de Dominicis.<sup>10</sup> Combescot and Nozières<sup>11</sup> have discussed the threshold behavior for potentials strong enough to bind an electron, which is closely related to the present work. A prior paper of ours<sup>12</sup> treated a model consisting of one narrow band interacting with a core hole, in conjunction with an analysis of the Hubbard model. The present work is a generalization and extension of that treatment.

The relevance of the core spectra to the valence-band photoemission from Ni has been discussed by us<sup>12,13</sup> and by Treglia *et al.*<sup>14</sup> It has been shown that the presence of a large  $3d$  satellite (similar to the satellite in the core spectra) implies a strong hole-hole interaction which, in turn, implies correlations that narrow the  $3d$  bands in Ni. Understanding the core problem is

a prerequisite to understanding the electronic structure of the valence bands. Eastman *et al.*<sup>15</sup> have summarized the results of extensive experimental and theoretical investigations of the electronic structure of the 3d metals; in Sec. IV of Ref. 15, Wendin presents an essentially atomic description of various core-level spectroscopies, including photoemission.

In Sec. II, the formalism for the interaction of multiple bands with a core hole is derived. Numerical results and comparison to experiment are presented in Sec. III. Our conclusions and discussion of other metals and related Auger experiments are presented in Sec. IV.

## II. FORMAL THEORY

In this section, we present the formal theory for the interaction of a core hole with the valence-band electrons of a narrow-band metal, such as Ni, including the computation of the core photoemission spectrum.

### A. One-electron wave functions

A hole in a core level produces a change  $\delta V$  in the self-consistent potential of the valence elec-

trons. This change includes not only the Hartree and exchange-correlation potentials due to the hole, but also the change due to the relaxation of the valence-band electrons towards the hole. Because of screening, we expect it to be large only in the unit cell containing the hole.

The Bloch functions describing the ground state can be written in a linear combination of atomic orbitals (LCAO) basis<sup>16</sup> for either spin<sup>17</sup> as

$$\psi_{\vec{k}n}(\vec{r}) = N^{-1/2} \sum_i e^{i\vec{k}\cdot\vec{R}_i} \sum_\gamma a_\gamma(\vec{k}n) w_\gamma(\vec{r} - \vec{R}_i), \quad (1)$$

where  $N$  is the number of lattice sites  $\vec{R}_i$ ,  $w_\gamma(\vec{r})$  is an atomiclike basis function (3d, 4s, 4p), and  $a_\gamma(\vec{k}n)$  is a coefficient which depends on wave vector  $\vec{k}$  and band index  $n$  ( $n$ th band at  $\vec{k}$ ). This formalism allows hybridization of the 3d bands with the 4s-4p bands. The  $w_\gamma(\vec{r})$  are orthonormal on a given site

$$\langle w_\gamma(\vec{r}) | w_{\gamma'}(\vec{r}) \rangle = \delta_{\gamma\gamma'}, \quad (2)$$

but there is some overlap between functions on different sites.

The matrix elements of  $\delta V$  are of the form

$$\langle \psi_{\vec{k}n} | \delta V | \psi_{\vec{k}'n'} \rangle = N^{-1} \sum_{ij} \exp(i\vec{k}'\cdot\vec{R}_j - i\vec{k}\cdot\vec{R}_i) \sum_{\gamma\gamma'} a_\gamma^*(\vec{k}n) a_{\gamma'}(\vec{k}'n') \langle w_\gamma(\vec{r} - \vec{R}_i) | \delta V | w_{\gamma'}(\vec{r} - \vec{R}_j) \rangle. \quad (3)$$

Taking  $\delta V$  to be spherically symmetric, we have for  $\vec{R}_i = \vec{R}_j = 0$  (core-hole site)

$$\langle w_\gamma(\vec{r}) | \delta V | w_{\gamma'}(\vec{r}) \rangle = 0, \quad \gamma \neq \gamma'. \quad (4)$$

(If 4d functions, for example, had been included in the basis set,  $\langle w_\gamma | \delta V | w_{\gamma'} \rangle$  would not necessarily be diagonal.) The largest and most important matrix elements involve the 3d functions. Let  $\gamma = 1, 2, \dots, 5$  refer to the five 3d functions (three of  $t_{2g}$  symmetry,  $xy$ ,  $yz$ , and  $zx$ ; two of  $e_g$  symmetry,  $x^2 - y^2$  and  $3z^2 - r^2$ ). In principle, the interaction for  $\gamma = \gamma' = t_{2g}$  can be different from  $\gamma = \gamma' = e_g$ . However, this is a small effect which is neglected here for simplicity. Also, we neglect on-site interactions for  $\gamma, \gamma' > 5$ . Therefore, we have

$$\langle w_\gamma(\vec{r}) | \delta V | w_\gamma(\vec{r}) \rangle = \begin{cases} -U, & \gamma = 1, 2, \dots, 5 \\ 0, & \gamma > 5. \end{cases} \quad (5a)$$

$$(5b)$$

$U$  can be regarded as a parameter which determines the strength of the interaction.

Matrix elements involving  $\vec{R}_i$  and/or  $\vec{R}_j \neq 0$  in (3) are small and are neglected except for func-

tions which overlap a 3d on the origin. For example, 4p functions on adjacent sites slightly overlap the 3d functions. We assume that it is the projection of the 4p function  $w_{4p}(\vec{r} - \vec{R}_i)$  on  $w_{3d}(\vec{r})$  that determines the strength of the interaction. A convenient form for  $\delta V$  which accounts for this overlap is

$$\delta V = -U \sum_{\beta=1}^5 |w_\beta(\vec{r})\rangle \langle w_\beta(\vec{r})|. \quad (6)$$

Substituting (6) into (3) gives

$$\langle \psi_{\vec{k}n} | \delta V | \psi_{\vec{k}'n'} \rangle = -(U/N) \sum_{\beta=1}^5 \bar{a}_\beta^*(\vec{k}n) \bar{a}_\beta(\vec{k}'n'), \quad (7)$$

where

$$\bar{a}_\beta(\vec{k}n) = \sum_\gamma O_{\beta\gamma}(\vec{k}) a_\gamma(\vec{k}n) \quad (8)$$

and

$$O_{\beta\gamma}(\vec{k}) = \sum_i \exp(i\vec{k}\cdot\vec{R}_i) \langle w_\beta(\vec{r}) | w_\gamma(\vec{r} - \vec{R}_i) \rangle. \quad (9)$$

The matrix  $O(\vec{k})$  is the Fourier transform of the overlap matrix. (Note that  $\sum_\gamma \dots$  is a sum over all basis functions 3d, 4s, and 4p, whereas  $\sum_{\beta=1}^5 \dots$  is over the 3d functions only.)

The orbitals in the presence of a core hole can be expanded as

$$\psi(\vec{r}) = \sum_{\vec{k}n} A_{\vec{k}n} \psi_{\vec{k}n}(\vec{r}). \quad (10)$$

From (7), we find the eigenvalue equation to be

$$(\epsilon_{\vec{k}n} - \omega) A_{\vec{k}n} = (U/N) \sum_{\beta=1}^5 \bar{a}_{\beta}^*(\vec{k}n) \sum_{\vec{k}'n'} \bar{a}_{\beta}(\vec{k}'n') A_{\vec{k}'n'}, \quad (11)$$

where  $\epsilon_{\vec{k}n}$  is the energy of the Bloch function  $\psi_{\vec{k}n}$ .

Let us first consider solutions of (11) for which  $\omega$  is not equal to any  $\epsilon_{\vec{k}n}$ . Then (11) can be written as

$$A_{\vec{k}n} = \frac{1}{\epsilon_{\vec{k}n} - \omega} \frac{U}{N} \sum_{\beta=1}^5 \bar{a}_{\beta}^*(\vec{k}n) \sum_{\vec{k}'n'} \bar{a}_{\beta}(\vec{k}'n') A_{\vec{k}'n'}. \quad (12)$$

Multiplying by  $\bar{a}_{\beta}(\vec{k}n)$ , summing over  $\vec{k}n$ , and defining

$$A_{\beta} \equiv \sum_{\vec{k}n} \bar{a}_{\beta}(\vec{k}n) A_{\vec{k}n}, \quad (13)$$

we find the equation

$$A_{\beta} = \frac{U}{N} \sum_{\beta'=1}^5 \sum_{\vec{k}n} \frac{\bar{a}_{\beta}(\vec{k}n) \bar{a}_{\beta'}^*(\vec{k}n)}{\epsilon_{\vec{k}n} - \omega} A_{\beta'}, \quad \beta=1, 2, \dots, 5. \quad (14)$$

Symmetry requires the sum over  $\vec{k}n$  to be zero if  $\beta' \neq \beta$ . Hence, the eigenvalues  $\omega$  are given by

$$1 = \frac{U}{N} \sum_{\vec{k}n} \frac{|\bar{a}_{\beta}(\vec{k}n)|^2}{\epsilon_{\vec{k}n} - \omega}, \quad \beta=1, 2, \dots, 5. \quad (15)$$

Equation (15) represents the solution of (11) by the Koster-Slater technique.<sup>18</sup>

For a given  $\beta$ , there are some  $\vec{k}n$  for which  $\bar{a}_{\beta}(\vec{k}n)$  vanishes and  $\epsilon_{\vec{k}n}$  does not appear in (15). Of those  $\vec{k}n$  which actually contribute to (15) for a given  $\beta$ , let  $\{\epsilon_1 < \epsilon_2 < \dots < \epsilon_M\}$  be the set of *distinct* values of  $\epsilon_{\vec{k}n}$ .<sup>19</sup> For each  $\epsilon_m$ , there is a solution  $\omega_m^{(\beta)}$  of (15) which lies between  $\epsilon_{m-1}$  and  $\epsilon_m$  (assuming  $U > 0$ ). The lowest solution,  $\omega_1^{(\beta)}$ , occurs below  $\epsilon_1$ .

From (12) and (13), we see that the corresponding normalized eigenvector is (note  $A_{\beta}^{(\beta, m)} = 0$ ,  $\beta' \neq \beta$ )

$$A_{\vec{k}n}^{(\beta, m)} = \frac{\bar{a}_{\beta}^*(\vec{k}n)}{\epsilon_{\vec{k}n} - \omega_m^{(\beta)}} \left( \sum_{\vec{k}'n'} \frac{|\bar{a}_{\beta}(\vec{k}'n')|^2}{(\epsilon_{\vec{k}'n'} - \omega_m^{(\beta)})^2} \right)^{-1/2}. \quad (16)$$

These solutions will be called the perturbed solutions and are written in real space as

$$\psi_m^{(\beta)}(\vec{r}) = \sum_{\vec{k}n} A_{\vec{k}n}^{(\beta, m)} \psi_{\vec{k}n}(\vec{r}). \quad (17)$$

Each solution transforms like a  $t_{2g}$  or an  $e_g$  function. Also,  $\omega_m^{(xy)} = \omega_m^{(yz)} = \omega_m^{(zx)}$  and  $\omega_m^{(x^2-y^2)} = \omega_m^{(3z^2-r^2)}$ .

The remaining solutions of (11) occur when  $\omega$  equals some  $\epsilon_{\vec{k}n}$ . These solutions satisfy

$$\sum_{\vec{k}'n'} \bar{a}_{\beta}(\vec{k}'n') A_{\vec{k}'n'} \Big|_{\epsilon_{\vec{k}'n'} = \epsilon_{\vec{k}n}} = 0, \quad (18)$$

where the sum is only over states with the same energy  $\epsilon_{\vec{k}n}$ . These are called the unperturbed solutions, which are the same for all values of  $U$  (including zero). They can be eliminated from the problem since they are passive orbitals, having the same occupancy in all excited states of interest as in the ground state. Note that the unperturbed orbitals are merely linear combinations of degenerate  $\psi_{\vec{k}n}$  and thus are eigenfunctions of the ground-state one-electron Hamiltonian. All purely  $4s-4p$  eigenfunctions (such as  $\Gamma_1$ ) fall into this category.

Returning to the perturbed solutions, we note that as  $U \rightarrow 0$ ,  $\omega_m^{(\beta)} \rightarrow \epsilon_m$ . From (16), we see that  $A_{\vec{k}n}^{(\beta, m)} \rightarrow 0$  unless  $\epsilon_{\vec{k}n} = \epsilon_m$  in which case

$$A_{\vec{k}n}^{(\beta, m)} \rightarrow \bar{a}_{\beta}^*(\vec{k}n) / (D_m^{(\beta)})^{1/2}, \quad (19)$$

where

$$D_m^{(\beta)} = \sum_{\vec{k}n} \left| \bar{a}_{\beta}(\vec{k}n) \right|^2 \Big|_{\epsilon_{\vec{k}n} = \epsilon_m} \quad (20)$$

The orbital associated with (19) (whose energy is  $\epsilon_m$ ) is

$$\psi_{m0}^{(\beta)}(\vec{r}) = (D_m^{(\beta)})^{-1/2} \sum_{\vec{k}n} \bar{a}_{\beta}^*(\vec{k}n) \psi_{\vec{k}n}(\vec{r}) \Big|_{\epsilon_{\vec{k}n} = \epsilon_m}, \quad (21)$$

which is a linear combination of degenerate  $\psi_{\vec{k}n}(\vec{r})$ . The  $\psi_{m0}^{(\beta)}(\vec{r})$  along with the unperturbed orbitals form a complete, orthonormal set related to the Bloch functions by a unitary transformation.

From (16), (17), and (21), we find that

$$\psi_m^{(\beta)}(\vec{r}) = \sum_{m'} \langle \psi_{m'0}^{(\beta)} | \psi_m^{(\beta)} \rangle \psi_{m'0}^{(\beta)}(\vec{r}), \quad (22)$$

where

$$\langle \psi_{m'0}^{(\beta)} | \psi_m^{(\beta)} \rangle = \frac{(D_m^{(\beta)})^{1/2}}{\epsilon_m - \omega_m^{(\beta)}} \left( \sum_{m''} \frac{D_{m''}^{(\beta)}}{(\epsilon_{m''} - \omega_m^{(\beta)})^2} \right)^{-1/2}. \quad (23)$$

From (1), (8), and (9), we find that

$$\bar{a}_{\beta}(\vec{k}n) = N^{1/2} \langle w_{\beta}(\vec{r}) | \psi_{\vec{k}n}(\vec{r}) \rangle. \quad (24)$$

Thus, we see from (20) that

$$D_m^{(\beta)} = N \sum_{\vec{k}n} \left| \langle w_{\beta}(\vec{r}) | \psi_{\vec{k}n}(\vec{r}) \rangle \right|^2 \Big|_{\epsilon_{\vec{k}n} = \epsilon_m}. \quad (25)$$

For  $m > 1$ , the orbitals  $\psi_m^{(\beta)}(\vec{r})$  correspond to scattering states. We can define a phase shift by

$$\delta_m^{(\beta)} = \pi \frac{\epsilon_m - \omega_m^{(\beta)}}{\epsilon_m - \epsilon_{m-1}}. \quad (26)$$

( $D_m^{(\beta)}$  and  $\epsilon_m - \epsilon_{m-1}$  must vary smoothly and reasonably slowly with  $m$  for this definition to be sensible.) It can be shown that this phase shift evaluated at the Fermi energy  $\epsilon_F$  gives the asymmetry parameter [x-ray photoemission spectroscopy (XPS) singularity index] for a single band<sup>6,11</sup>:  $\Delta = (\delta/\pi)^2$  (denoted by  $\alpha$  in Hüfner and Wertheim<sup>1</sup>).

For large enough  $U$ ,  $\omega_1^{(\beta)}$  corresponds to an orbital split off from the bottom of the band (bound state). The criterion is that there exists a solution  $\omega_1^{(\beta)}$  to the equation

$$1 = U \int \frac{d\epsilon n_\beta(\epsilon)}{\epsilon - \omega}, \quad (27)$$

where  $\omega_1^{(\beta)}$  is below the bottom of the  $3d$  bands. The  $\beta$ th partial density of states is given by [from (15) and (24)]

$$n_\beta(\epsilon) = N^{-1} \sum_{\vec{k}n} |\tilde{a}_\beta(\vec{k}n)|^2 \delta(\epsilon - \epsilon_{\vec{k}n}) \quad (28a)$$

$$= \sum_{\vec{k}n} |\langle w_\beta(\vec{r}) | \psi_{\vec{k}n}(\vec{r}) \rangle|^2 \delta(\epsilon - \epsilon_{\vec{k}n}). \quad (28b)$$

Note that  $\int d\epsilon n_\beta(\epsilon) = 1$ . The phase shift  $\delta_m^{(\beta)} = \delta_\beta(\epsilon_m)$  is related to  $n_\beta(\epsilon)$  by the formula<sup>10</sup>

$$\tan \delta_\beta(\epsilon) = \pi n_\beta(\epsilon) U / \left( 1 - U P \int n_\beta(\epsilon') d\epsilon' / (\epsilon' - \epsilon) \right), \quad (29)$$

where  $P$  denotes the principal value. In the limit  $U \rightarrow \infty$ ,  $\omega_1^{(\beta)} \rightarrow \bar{\epsilon}_\beta - U$ , where  $\bar{\epsilon}_\beta = \int \epsilon n_\beta(\epsilon) d\epsilon$ , and from (16) and (24) we have

$$\psi_1^{(\beta)}(\vec{r}) \rightarrow w_\beta(\vec{r}). \quad (30)$$

In this limit there are five orbitals  $\beta = 1, 2, \dots, 5$  (for each spin) split off from the bottom of the  $3d$  bands; these approach the  $3d$  basis functions on the core-hole site.

#### B. System states and photoemission

The system states in the presence of the core hole are products of wave functions, each of which represents a particular spin  $\sigma$  and basis function

$$\langle \Phi_g^{(\sigma, \beta)} | \phi^{(\sigma, \beta)} \rangle = \begin{vmatrix} \langle \psi_{1\sigma}^{(\beta)} | \psi_{m_1}^{(\beta)} \rangle & \langle \psi_{1\sigma}^{(\beta)} | \psi_{m_2}^{(\beta)} \rangle & \dots & \langle \psi_{1\sigma}^{(\beta)} | \psi_{m_L}^{(\beta)} \rangle \\ \langle \psi_{2\sigma}^{(\beta)} | \psi_{m_1}^{(\beta)} \rangle & \langle \psi_{2\sigma}^{(\beta)} | \psi_{m_2}^{(\beta)} \rangle & \dots & \langle \psi_{2\sigma}^{(\beta)} | \psi_{m_L}^{(\beta)} \rangle \\ \dots & \dots & \dots & \dots \\ \langle \psi_{L\sigma}^{(\beta)} | \psi_{m_1}^{(\beta)} \rangle & \langle \psi_{L\sigma}^{(\beta)} | \psi_{m_2}^{(\beta)} \rangle & \dots & \langle \psi_{L\sigma}^{(\beta)} | \psi_{m_L}^{(\beta)} \rangle \end{vmatrix}. \quad (38)$$

$\beta$ :

$$|\Phi\rangle = \prod_{\sigma=-1/2}^{1/2} \prod_{\beta=1}^5 |\phi^{(\sigma, \beta)}\rangle, \quad (31)$$

where  $|\phi^{(\sigma, \beta)}\rangle$  stands for a Slater determinant of  $L$  orbitals  $\psi_m^{(\beta)}(\vec{r})$  with spin  $\sigma$ ,  $m = m_1, m_2, \dots, m_L$ . The total energy  $E_\Phi$  associated with  $|\Phi\rangle$  is

$$E_\Phi = \sum_{\sigma=-1/2}^{1/2} \sum_{\beta=1}^5 E^{(\sigma, \beta)}, \quad (32)$$

where

$$E^{(\sigma, \beta)} = \sum_{i=1}^L \omega_{m_i}^{(\beta)}. \quad (33)$$

To avoid unnecessarily complicated formulas, we have not included a spin index on  $\omega_m^{(\beta)}$  or a  $(\sigma, \beta)$  index on  $L$ . Also, it is always understood that the set  $\{m_1, m_2, \dots, m_L\}$ , which we denote by  $\alpha^{(\sigma, \beta)}$ , can be different for each  $(\sigma, \beta)$ . Hence, each system state  $\Phi$  is specified by ten sets  $\alpha^{(\sigma, \beta)}$ . We have eliminated the unperturbed orbitals since they are passive.

The ground state (no core hole) can be written in a similar fashion as follows:

$$|\Phi_g\rangle = \prod_{\sigma=-1/2}^{1/2} \prod_{\beta=1}^5 |\Phi_g^{(\sigma, \beta)}\rangle, \quad (34)$$

where  $|\Phi_g^{(\sigma, \beta)}\rangle$  represents a Slater determinant of  $L$  orbitals  $\psi_{m\sigma}^{(\beta)}(\vec{r})$  with spin  $\sigma$ . Let these orbitals be denoted by  $m = 1, 2, \dots, L$ . Of course,  $\epsilon_m < \epsilon_F$  for  $m = 1, 2, \dots, L$  and  $\epsilon_m > \epsilon_F$  for  $m > L$ .<sup>19</sup> If, as assumed here, the ground-state orbitals with the same energy are either all occupied or all empty (never partially occupied), the present description of the ground state is equivalent to the usual procedure in which the occupancy of Bloch orbitals  $\psi_{\vec{k}n}$  is specified. The ground-state energy is

$$E_g = \epsilon_c + \sum_{\sigma=-1/2}^{1/2} \sum_{\beta=1}^5 E_g^{(\sigma, \beta)}, \quad (35)$$

where  $\epsilon_c$  is the energy of the core level and

$$E_g^{(\sigma, \beta)} = \sum_{m=1}^L \epsilon_m. \quad (36)$$

In the sudden approximation, the probability of excitation of  $\Phi$  in photoemission is

$$|\langle \Phi_g | \Phi \rangle|^2 = \prod_{\sigma=-1/2}^{1/2} \prod_{\beta=1}^5 |\langle \Phi_g^{(\sigma, \beta)} | \phi^{(\sigma, \beta)} \rangle|^2. \quad (37)$$

It is straightforward to show that

The elements of the determinant can be evaluated using (23). Conservation of energy requires that

$$E_K + E_\phi = h\nu + E_g. \quad (39)$$

where  $E_K$  is the kinetic energy of the photoelectron and  $h\nu$  is the photon energy. Hence, the photoemission intensity is proportional to the spectral density function

$$\rho^0(\epsilon) = \sum_{\Phi} |\langle \Phi_g | \Phi \rangle|^2 \delta(\epsilon - E_\Phi + E_g), \quad (40)$$

where the sum is over all excited states and the binding energy  $\epsilon$  is given by

$$\epsilon = h\nu - E_K. \quad (41)$$

Equation (40) can be evaluated upon substitution of Eqs. (32), (35), and (37). We note that  $\rho^0(\epsilon)$  is a multiple convolution of individual spectral density functions, one for each  $(\sigma, \beta)$ :

$$\rho^{(\sigma, \beta)}(x) = \sum_{\alpha^{(\sigma, \beta)}} |\langle \Phi_g^{(\sigma, \beta)} | \phi^{(\sigma, \beta)} \rangle|^2 \delta(x - E^{(\sigma, \beta)} + E_g^{(\sigma, \beta)}), \quad (42)$$

where the sum is over all sets  $\alpha^{(\sigma, \beta)} = \{m_1, m_2, \dots, m_L\}$ , with  $(\sigma, \beta)$  fixed.

### C. Sum rules

It is useful to derive sum rules for the spectral density function  $\rho^0(\epsilon)$ . Let the  $n$ th moment about  $-\epsilon_c = |\epsilon_c|$  be (recall that, in  $\rho^0(\epsilon)$ ,  $\epsilon$  is a binding energy)

$$M_n \equiv \int d\epsilon \rho^0(\epsilon) (\epsilon + \epsilon_c)^n. \quad (43)$$

From (40), we have

$$M_n = \sum_{\Phi} |\langle \Phi_g | \Phi \rangle|^2 (E_\Phi + \epsilon_c - E_g)^n. \quad (44)$$

From (32) and (35), we find for  $n=0, 1$ , and 2

$$M_n = \langle \Phi_g | H_{\text{int}}^n | \Phi_g \rangle, \quad (45)$$

where  $H_{\text{int}}$  is a one-body operator of the form (in second quantized notation)

$$H_{\text{int}} = \sum_{\sigma=-1/2}^{1/2} \sum_{\vec{k}n} \sum_{\vec{k}'n'} \langle \psi_{\vec{k}n\sigma} | \delta V | \psi_{\vec{k}'n'\sigma} \rangle c_{\vec{k}n\sigma}^\dagger c_{\vec{k}'n'\sigma}, \quad (46)$$

$c_{\vec{k}n\sigma}^\dagger$  is a creation operator for the orbital  $\psi_{\vec{k}n\sigma}$ , and  $\delta V$  is the hole-valence band interaction (6).

For  $n=0$ , (45) gives

$$M_0 = 1, \quad (47)$$

i.e.,  $\rho^0(\epsilon)$  is normalized to unity. The mean ( $n=1$ ) can be found from (7) to be

$$M_1 = -(U/N) \sum_{\beta=1}^5 \sum_{\vec{k}n\sigma} |\tilde{a}_\beta(\vec{k}n\sigma)|^2 f_{\vec{k}n\sigma}, \quad (48)$$

where  $f_{\vec{k}n\sigma} = 1$  (0) for orbitals occupied (empty) in the ground state. From (28), we find that

$$M_1 = -U \sum_{\beta=1}^5 \sum_{\sigma=-1/2}^{1/2} N_{\beta\sigma}, \quad (49)$$

where the fractional filling  $N_{\beta\sigma}$  is given by

$$N_{\beta\sigma} = \int_{-\infty}^{\epsilon_F} n_{\beta\sigma}(\epsilon) d\epsilon, \quad (50)$$

and we have given  $n_\beta(\epsilon)$  an explicit spin index.

In a similar manner, one can show that for each  $(\sigma, \beta)$

$$\int \rho^{(\sigma, \beta)}(x) dx = 1, \quad (51)$$

and

$$\int x \rho^{(\sigma, \beta)}(x) dx = -UN_{\beta\sigma}. \quad (52)$$

## III. NUMERICAL RESULTS

### A. Equivalent eigenvalue problem

The perturbed solutions are given by (15) and (16). The quantities  $\omega_m^{(\beta)}$  and  $A_{kn}^{(\beta, m)}$  can be determined numerically from these equations. However, sometimes we have found it convenient to solve directly an equivalent eigenvalue problem. Let us rewrite (15) using (20) (again suppressing the  $\sigma$  index),

$$1 = \frac{U}{N} \sum_m \frac{D_m^{(\beta)}}{\epsilon_m - \omega}. \quad (53)$$

Consider the eigenvalue problem [for a given  $(\sigma, \beta)$ ]

$$\sum_{m'} H_{mm'}^{(\beta)} R_{m'} = \omega R_m, \quad (54)$$

where

$$H_{mm'}^{(\beta)} = \epsilon_m \delta_{mm'} - (U/N) (D_m^{(\beta)} D_{m'}^{(\beta)})^{1/2}. \quad (55)$$

(Note that  $H_{mm'}^{(\beta)}$  is a matrix of order  $M$ .) Using the Koster-Slater technique,<sup>18</sup> it is straightforward to verify that the eigenvalues of (54) are identical to those of (53). Furthermore, the  $m$ th eigenvector is [from (23)]

$$R_m^{(\beta, m)} = \langle \psi_{m'o}^{(\beta)} | \psi_m^{(\beta)} \rangle. \quad (56)$$

Therefore, (38) becomes

$$\langle \Phi_g^{(\sigma, \beta)} | \phi^{(\sigma, \beta)} \rangle = \begin{vmatrix} R_1^{(\beta, m_1)} & R_1^{(\beta, m_2)} & \dots & R_1^{(\beta, m_L)} \\ R_2^{(\beta, m_1)} & R_2^{(\beta, m_2)} & \dots & R_2^{(\beta, m_L)} \\ \dots & \dots & \dots & \dots \\ R_L^{(\beta, m_1)} & R_L^{(\beta, m_2)} & \dots & R_L^{(\beta, m_L)} \end{vmatrix}. \quad (57)$$

For this method to be tractable in actual practice, we must have  $M \leq 10^2$ . Equations (53)–(57) along with (20) provide a method by which to choose the mesh, i.e., to choose the  $\epsilon_m$ 's. For each  $(\sigma, \beta)$ , we imagine dividing the energy range over which  $n_\beta(\epsilon)$  is nonzero into intervals  $\Delta\epsilon_m$ ,  $m = 1, 2, \dots, M$ . All  $\epsilon_{kn}$  falling into the  $m$ th interval are replaced by the same energy  $\epsilon_m$ . Hence, all but one level in the interval can be eliminated from the problem since they can be treated as passive orbitals which give unperturbed solutions. The remaining level gives a perturbed solution.

The quantity  $D_m^{(\beta)}$  has the entire "weight" of the interval. According to (20) and (28), we take

$$\int_{\Delta\epsilon_m} n_\beta(\epsilon) d\epsilon = D_m^{(\beta)} / N. \quad (58)$$

Also, we choose

$$\int_{\Delta\epsilon_m} \epsilon n_\beta(\epsilon) d\epsilon / \int_{\Delta\epsilon_m} n_\beta(\epsilon) d\epsilon = \epsilon_m. \quad (59)$$

The evaluation of the determinant can be accomplished by noting from (23), (56), and (57) that [omitting the  $(\sigma, \beta)$  superscripts]

$$\langle \Phi_g | \phi \rangle = \frac{\prod_{m=1}^L D_m^{1/2}}{\prod_{i=1}^L \left( \sum_{j=1}^N \frac{D_j}{(\epsilon_j - \omega_{m_i})^2} \right)^{1/2}} \begin{vmatrix} (\epsilon_1 - \omega_{m_1})^{-1} & (\epsilon_1 - \omega_{m_2})^{-1} & \dots & (\epsilon_1 - \omega_{m_L})^{-1} \\ (\epsilon_2 - \omega_{m_1})^{-1} & (\epsilon_2 - \omega_{m_2})^{-1} & \dots & (\epsilon_2 - \omega_{m_L})^{-1} \\ \dots & \dots & \dots & \dots \\ (\epsilon_L - \omega_{m_1})^{-1} & (\epsilon_L - \omega_{m_2})^{-1} & \dots & (\epsilon_L - \omega_{m_L})^{-1} \end{vmatrix}. \quad (60)$$

To the determinant in (60), we may apply the following algorithm given by Pólya and Szegő<sup>20</sup>:

$$\left| \frac{1}{\epsilon_\lambda - \omega_{m_\mu}} \right|_1^L = \frac{\prod_{j>k}^{1,2,\dots,L} (\epsilon_j - \epsilon_k)(\omega_{m_k} - \omega_{m_j})}{\prod_{\lambda,\mu}^{1,2,\dots,L} (\epsilon_\lambda - \omega_{m_\mu})}. \quad (61)$$

#### B. Application to Ni metal core levels

The simplest application of the present theory has been presented in Sec. II of Ref. 12. In that paper we considered only a single band of spin  $\downarrow$  (i.e.,  $\beta = 1, \sigma = \downarrow$ ). The density of states  $n_\rho(\epsilon)$  was taken to be uniform for  $|\epsilon| < W/2$ , where  $W$  is the bandwidth. The resulting spectrum  $\rho^0(\epsilon)$  consists of two parts, a main line and a satellite. The threshold for the main line corresponds to the lowest  $L$  of the  $\omega_m$  being occupied. The satellite threshold is at a binding energy  $\epsilon$  which is higher by  $\omega_{L+1} - \omega_1$ , that is, the bound state is not occupied. On the high-binding-energy side of each threshold is a tail due to the creation of electron-hole pairs. The approach to threshold of  $\rho^0(\epsilon)$  is described by asymptotic theory.<sup>6,10,11</sup>

In the case of multiple bands, the spectrum  $\rho^0(\epsilon)$  is a convolution of individual  $\rho^{(\sigma,\beta)}(\epsilon)$ , each of which has a form similar to that described above. However, the individual spectra  $\rho^{(\sigma,\beta)}(\epsilon)$  differ in one respect from that obtained in Ref. 12. Due to the  $s$ - $d$  interaction, the  $n_\beta(\epsilon)$  do not have an abrupt lower edge but tail off gradually. Consequently the satellite is spread out and does not have as sharp a threshold as in the simple model.

Since the  $3d\uparrow$  bands are essentially full in Ni, their contribution to the core line shape can be neglected. Likewise, since the core-hole interaction with the  $4s$ - $4p$  bands has been neglected in our calculation, they too make no contribution to the line shape [aside from contributing to  $\tilde{\alpha}_\beta(kn)$ ]. We consider only the spin  $\downarrow$   $t_{2g}$  and  $e_g$  partial densities of states. The final spectrum  $\rho^0(\epsilon)$  is a convolution of three identical  $\rho^{(\downarrow, t_{2g})}(\epsilon)$  with two identical  $\rho^{(\downarrow, e_g)}(\epsilon)$ . To generate the partial densities of states  $n_{t_{2g}}(\epsilon)$  and  $n_{e_g}(\epsilon)$ , we used the LCAO model of Dempsey *et al.*,<sup>16</sup> parametrized to fit the bands of Wang and Callaway<sup>21</sup> (von Barth-Hedin potential). The parameter  $U$  was chosen to be 4 eV, which resulted in the satellite being  $\sim 6$  eV higher in binding energy than the main line. Each  $n_\rho(\epsilon)$  was divided into 76 levels, i.e.,  $M = 76$ , most of which had weight  $D_m^{(\beta)} / N = \frac{1}{63}$ . The resulting spectrum is shown as a histogram in Fig. 1. The resolution in binding energy is 0.1 eV. Each  $\rho^{(\downarrow, \beta)}(\epsilon)$  includes all single electron-hole pairs and all significant double pairs, giving a total intensity of 0.988 (out of 1.0). The remaining intensity is in triple (and higher-order) pairs. The main line contains about 75% of the intensity.

The main line corresponds to a local configuration of core hole plus  $d^{10}$ ; that is, with  $s$ - $d$  interaction neglected, there are five  $\downarrow$  bound states at the core site which are filled, in addition to the five  $\uparrow$  electrons from the filled  $3d\uparrow$  bands. For large enough  $U$ , a bound state is the same as an atomic basis function [see (30)] and Ni is close to this limit. The satellite corresponds to a core hole plus  $d^9$ , since one of the bound

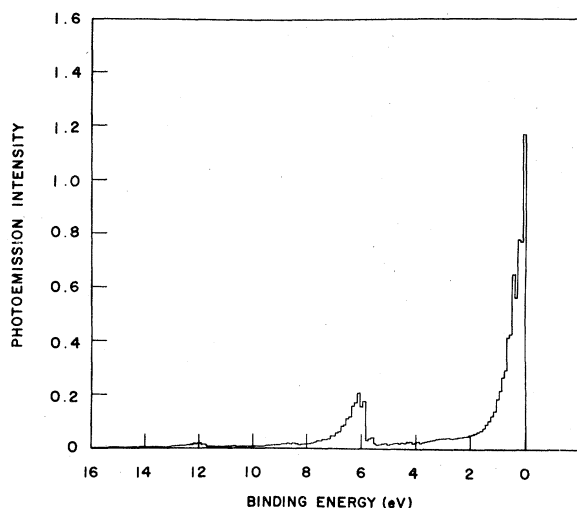


FIG. 1. Computed spectral density function of a core level in Ni metal as a function of binding energy relative to threshold. The interaction strength  $U$  was chosen to be 4 eV.

levels is unoccupied. Presumably the  $4s-4p$  charge density adjusts to maintain charge neutrality in a volume of the order of the unit cell. At  $\sim 12$  eV above the main line, a weak satellite appears in Fig. 1 corresponding to two bound levels unoccupied, i.e., the  $d^8$  configuration. In fact, all configurations  $d^n$ ,  $n = 5$  to 10 are represented. The energies of these higher-order satellites are not given correctly here, since the  $3d$  hole-hole repulsion has been neglected. Further, the multiplet structure of the satellite has been omitted. For example, if the core hole were  $3p$ , one would expect to see the  $3p^5 3d^9$  multiplets.

In Fig. 2, the spectrum of Fig. 1, convoluted with a Lorentzian of full width at half maximum (FWHM) =  $2\Gamma = 0.94$  eV, is compared to the  $2p_{3/2}$  core photoemission data of Hüfner and Wertheim<sup>1</sup> and that of Kowalczyk.<sup>2</sup> The value of  $\Gamma$  chosen is that given in Ref. 1 and represents the effects of the core-hole lifetime. The experimental curves contain background intensity which has not been removed. The qualitative features are in good agreement with the calculation. Although it is difficult to judge how much of the tail is background and how much intrinsic, the calculated strength of the satellite appears to be consistent with the data. The satellite is broader than calculated, perhaps due to multiplet effects which have been omitted. Comparison of experimental and calculated asymmetry of the main line is best assessed in Fig. 3.

Hüfner and Wertheim were able to fit their data with a function consisting of three parts. The first was of the Doniach-Sunjc form<sup>6</sup> for the

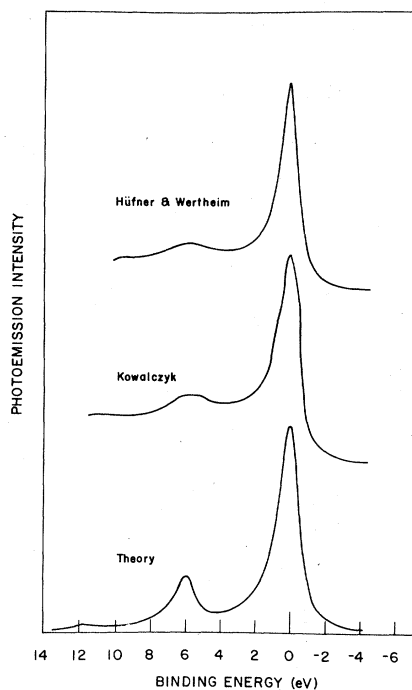


FIG. 2. Computed spectral density function (shown in Fig. 1) convoluted with a Lorentzian ( $2\Gamma = 0.94$  eV) versus binding energy. Experimental  $2p_{3/2}$  core-level x-ray photoemission spectra of Hüfner and Wertheim (Ref. 1) and Kowalczyk (Ref. 2) are shown for comparison. No background has been subtracted from the data.

main line given by asymptotic theory:

$$I(\epsilon) \sim \cos\left[\frac{1}{2}\pi\Delta + \Theta(\epsilon)\right] / (\epsilon^2 + \Gamma^2)^{(1-\Delta)/2}, \quad (62a)$$

where

$$\Theta(\epsilon) = - (1 - \Delta) \tan^{-1}(\epsilon/\Gamma), \quad (62b)$$

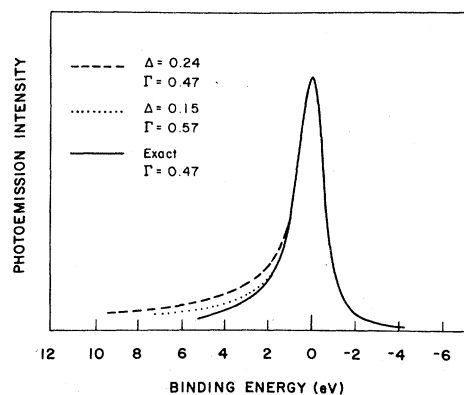


FIG. 3. Computed main-line intensity (solid curve) compared to the Doniach-Sunjc form (Ref. 6). The dashed curve is the fit to data obtained by Hüfner and Wertheim (Ref. 1).  $\Delta$  (denoted by  $\alpha$  in Ref. 1) = 0.24 and  $2\Gamma = 0.94$  eV. The dotted curve is a better fit to the computed intensity:  $\Delta = 0.15$  and  $2\Gamma = 1.14$  eV.

and  $\epsilon$  is measured relative to threshold (in the absence of broadening). The asymmetry parameter  $\Delta$  was found to be 0.24 for  $2p_{1/2}$  and  $2p_{3/2}$  (0.22 for  $3s$ , 0.18 for  $3p_{1/2}$ , and 0.23 for  $3p_{3/2}$ ).<sup>1</sup> The second part was a Lorentzian representing the satellite, and the third was a linear background.<sup>22</sup> In Fig. 3, we compare just that part given by (62) to our calculated main-line intensity folded with a Lorentzian with  $\Gamma = 0.47$  (solid line). The main line is defined as all intensity in Fig. 1 with binding energy  $\epsilon < 5.6$  eV. In Fig. 3, the form (62) is multiplied by a constant such that the peak values agree, and the origin is adjusted so that the peaks occur at the same  $\epsilon$ . The dashed curve is for the parameters that Hüfner and Wertheim found from their data. The dotted curve is for  $\Delta = 0.15$  and  $\Gamma = 0.57$ , which fits the calculated spectrum somewhat better. Hence we see that our calculated curve gives less asymmetry than measured, but still a reasonable amount. If the other bands (such as  $4s-4p$ ) had been included, the asymmetry would have been larger. The phase shifts at the Fermi level are calculated to be  $\delta_{t_{2g}} = 0.49\pi$  and  $\delta_{e_g} = 0.26\pi$  for  $U = 4$  eV and the Ni band structure. The value of  $\Delta$  from asymptotic theory is  $3(\delta_{t_{2g}}/\pi)^2 + 2(\delta_{e_g}/\pi)^2 = 0.86 \pm 0.03$ . For the interaction and band structure used in this paper, the asymptotic theory holds for only a small region, so that the effective  $\Delta$  ( $\sim 0.15$ ) is much different.

However, the physical significance of our calculated  $\Delta$  is questionable. From the Friedel sum rule, the charge induced around the core hole is  $3\delta_{t_{2g}}/\pi + 2\delta_{e_g}/\pi = 2.0$  electrons. This implies that the  $3d$  bands overscreen by one unit of charge. No more than  $\sim 0.9$  of the induced charge can occur at the site of the core hole in our model, since the  $3d\uparrow$  bands contain  $\sim 4.1$  electrons per site and the local charge configuration corresponds to five  $3d\uparrow$  electrons. The remaining 1.1 electrons are on neighboring sites. The magnitude of  $U$  is not the primary source of the difficulty; for  $U = 2.5$  eV, the induced charge is still  $\sim 1.8$ . Some of the excess induced charge is probably compensated by the  $4s-4p$  bands (negative phase shift giving an induced charge of the opposite sign). An additional explanation is that the neighboring sites have slightly repulsive potentials due to the pileup of  $3d$  charge. This has the effect of reducing the phase shift at the Fermi level and consequently the screening without significantly altering the position and strength of the satellite. Although the detailed line shape changes at threshold, the effect away from threshold should not be extremely large. We have performed simple one-dimensional calculations which support these conclusions.

Tersoff *et al.*<sup>7,8</sup> have used a  $t$ -matrix approach to analyze a model which is quite similar to ours. Their intraband interaction parameter  $V_1$  is roughly equivalent to  $U$  in our calculation. However, they must assume a value  $V_1 = 10$  eV for the satellite binding energy to be 5.1 eV larger than the main line, whereas we find that  $U = 4$  eV gives 6 eV. The discrepancy can be traced to an expression for the energy of the bound state. Equation (27) gives  $\omega = \omega_1^{(B)}$  in terms of  $U$  and the density of states. The analogous equation in Tersoff *et al.* erroneously contains a factor (which is 0.4) representing the occupancy of the bands.

#### IV. CONCLUSIONS AND DISCUSSION

In Sec. III, we compared our results to the  $2p_{3/2}$  core line of Ni. Except for differences due to  $\Gamma$  or to multiplet splittings, other core lines should be similar according to our theory because  $U$ , the only free parameter, must be roughly the same for all. That  $U$  must be the same follows from the observation that the satellite binding energy is  $\sim 6$  eV higher than the main line in all cases.<sup>3</sup> Hüfner and Wertheim<sup>1</sup> found similar values of the asymmetry parameter  $\Delta$  for all lines in Ni, which also indicates that  $U$  is about the same, since  $\Delta$  depends only upon  $U$  and the density of states. The data show that, apart from background, the  $2p_{1/2}$  line is similar to  $2p_{3/2}$  but with a larger  $\Gamma$ . The  $3s$  line is also similar, but with an even larger  $\Gamma$ .

The  $3p$  lines are interesting in that the satellite shows the multiplet splitting appropriate to the  $3p^5 3d^9$  configuration. This is evident from a comparison to the  $L_3 M_{23} M_{45}$  Auger spectrum of Yin *et al.*<sup>23</sup> on Ni metal. The  $L_3 M_{23} M_{45}$  transitions result in final states with the  $3p^5 3d^9$  configuration. The satellite, like the Auger spectrum, consists of two peaks. The peak at the higher binding energy is due to  $3p^5 3d^9$  ( $^1F$ ,  $^1P$ ) and the peak at lower energy is due to  $^3D$  and  $^3P$ . The  $^1D$  and  $^3F$  multiplets are weak in Auger. In XPS, these final states are not necessarily weak but they overlap the main line. The energies of the states agree between the two experiments and confirm the interpretation. The  $2p$  multiplets are split less than the  $3p$  since the relevant Slater integrals are less.<sup>24</sup> In addition, the multiplet structure in  $jj$  coupling ( $2p$ ) is different from that for  $LS$  ( $3p$ , where the spin-orbit interaction is much weaker) and not so spread out for a given  $j$ . Hence, no multiplets are resolved in the  $2p$  satellite.

In Ni metal, we conclude that the simple model presented in this paper gives an adequate description of core photoemission. The physical picture is also consistent with the  $L_3 M_{23} M_{45}$

Auger spectrum.

In the metals with higher  $Z$  (Cu, Zn, ...), the model presented here also applies. The satellite is, however, very weak since the  $3d$  bands are essentially full, and the requisite  $d$ -band shake-up transitions are improbable. However, the two-hole bound state ( $3p^5 3d^9$  configuration) is a well-defined excitation and it is the preferred final state for Auger processes. Sawatzky<sup>25</sup> and Cini<sup>26</sup> have demonstrated how it is possible to have two bound holes in metals with filled narrow bands. They specifically considered the  $3d^8$  configuration, but the arguments also apply to  $3p^5 3d^9$ . In this limit, our model is equivalent to theirs, apart from the consideration of multiple bands and multiplets.

For the transition metals with lower  $Z$  (Co, Fe, ...) the situation is less clear. Since  $U$  apparently becomes smaller<sup>23,27</sup> and the bands become wider, the splitoff level at  $\omega_1^{(B)}$  may no longer be bound. This is consistent with the satellite generally being much weaker or nonexistent. The  $L_3 M_{23} M_{45}$  spectra of Co, Fe, ... tend to overlap the two-hole continuum (one hole in the  $3p$  level and one free hole in the  $3d$  band whose energy can be anywhere from  $\epsilon_F$  to the bottom of the band), which indicates that the two-hole bound state is only weakly bound or becomes a resonance. A puzzling feature of the spectra is that for Fe, and to a greater extent Co, there are two peaks as in Ni, although the peaks are broader and less well defined. One would not expect to

see the  $3p^5 3d^9$  multiplets in Fe (whose ground state is  $\sim 3d^7 4s^1$ ). One explanation, which seems unlikely, is that the main line in Co XPS is roughly  $3p^5 3d^{10}$  with no  $4s$ - $4p$  screening, while the satellite and Auger peaks are  $3p^5 3d^9$  with some  $4s$ - $4p$  screening. None of the  $2p$  or  $3p$  XPS main lines show any multiplet splitting other than spin-orbit. Conceivably the two peaks in the Co and Fe Auger spectra are not due to multiplets, but instead represent a band-structure and/or matrix-element effect. Another possibility is that the peak at lower binding energy corresponds to the continuum and the other peak is a bound (or resonance) two-hole contribution. An accurate measurement of the binding energies would be helpful in this regard.

To further complicate the situation, the  $2s$  and  $3s$  XPS lines have what appear to be satellites (or at least shoulders).<sup>2</sup> The satellite is well defined in Fe and is still evident in Cr. It has been suggested that the two peaks represent exchange-split main lines modified by correlation effects. Kowalczyk<sup>2</sup> has discussed this interpretation, but did not reach a definite conclusion as to its validity. For Ni, we would regard our model as being more applicable.

#### ACKNOWLEDGMENTS

The authors would like to thank J. D. Dow, D. R. Penn, G. Sawatzky, B. Sonntag, G. Wendin, and G. W. Wertheim for helpful discussions and/or correspondence.

<sup>1</sup>S. Hüfner and G. W. Wertheim, Phys. Lett. **51A**, 301 (1975).

<sup>2</sup>S. P. Kowalczyk, Ph.D. thesis, University of California, Berkeley, 1976 (unpublished).

<sup>3</sup>S. Hüfner and G. W. Wertheim, Phys. Lett. **51A**, 299 (1975).

<sup>4</sup>S. Hüfner, G. W. Wertheim, and J. H. Wernick, Solid State Commun. **17**, 417 (1975).

<sup>5</sup>A. Kotani and Y. Toyozawa, J. Phys. Soc. Jpn. **37**, 912 (1974).

<sup>6</sup>S. Doniach and M. Sunjic, J. Phys. C **3**, 285 (1970).

<sup>7</sup>J. Tersoff, L. M. Falicov, and D. R. Penn, Solid State Commun. **32**, 1045 (1979).

<sup>8</sup>The calculated binding energy of the satellite is in error in Ref. 7. D. R. Penn (private communication).

<sup>9</sup>C. A. Swarts, J. D. Dow, and C. P. Flynn, Phys. Rev. Lett. **43**, 158 (1979); J. D. Dow, Nuovo Cimento **39B**, 465 (1977); J. D. Dow and C. P. Flynn, J. Phys. C **13**, 1341 (1980).

<sup>10</sup>P. Nozières and C. T. de Dominicis, Phys. Rev. **178**, 1097 (1969).

<sup>11</sup>M. Combescot and P. Nozières, J. Phys. (Paris) **32**, 913 (1971).

<sup>12</sup>L. C. Davis and L. A. Feldkamp, J. Appl. Phys. **50**,

Pt. 2, 1944 (1979).

<sup>13</sup>L. C. Davis and L. A. Feldkamp, Solid State Commun. **34**, 141 (1980).

<sup>14</sup>G. Treglia, F. Ducastelle, and D. Spanjaard, Phys. Rev. B **21**, 3729 (1980).

<sup>15</sup>D. E. Eastman, J. F. Janak, A. R. Williams, R. V. Coleman, and G. Wendin, J. Appl. Phys. **50**, Pt. 2, 7423 (1979). This paper contains numerous references not explicitly discussed here.

<sup>16</sup>D. G. Dempsey, W. R. Grise, and L. Kleinman, Phys. Rev. B **18**, 1270 (1978).

<sup>17</sup>Throughout Sec. IIA we suppress the spin label  $\sigma$ . In principle, the wave function, etc. can depend upon spin.

<sup>18</sup>G. F. Koster and J. C. Slater, Phys. Rev. **95**, 1167 (1954).

<sup>19</sup>The set of  $\epsilon_m$  is not necessarily the same for each  $(\sigma, \beta)$ .

<sup>20</sup>G. Pólya and G. Szegő, *Aufgabe und Lehrsätze aus der Analysis* (Dover, New York, 1945), Vol. 2, p. 48.

<sup>21</sup>C. S. Wang and J. Callaway, Phys. Rev. B **15**, 298 (1977).

<sup>22</sup>G. W. Wertheim (private communication).

<sup>23</sup>L. I. Yin, T. Tsang, and I. Adler, Phys. Rev. B **15**,

2974 (1977).

<sup>24</sup>J. B. Mann, Los Alamos Scientific Laboratory Report No. AEC-LA-3690 (unpublished).

<sup>25</sup>G. A. Sawatzky, Phys. Rev. Lett. 39, 504 (1977). Also see G. A. Sawatzky and A. Lenselink, Phys. Rev. B 21,

1790 (1980).

<sup>26</sup>M. Cini, Solid State Commun. 24, 681 (1977); Phys. Rev. B 17, 2788 (1978).

<sup>27</sup>E. Antonides, E. C. Janse and G. A. Sawatzky, Phys. Rev. B 15, 1669 (1977).